



University of HUDDERSFIELD

University of Huddersfield Repository

Jones, Benjamin and Barklie, R.C.

Electron paramagnetic resonance evaluation of defects at the (100)Si/Al₂O₃ interface

Original Citation

Jones, Benjamin and Barklie, R.C. (2005) Electron paramagnetic resonance evaluation of defects at the (100)Si/Al₂O₃ interface. *Journal of Physics D: Applied Physics*, 38 (8). pp. 1178-1181. ISSN 0022-3727

This version is available at <http://eprints.hud.ac.uk/19309/>

The University Repository is a digital collection of the research output of the University, available on Open Access. Copyright and Moral Rights for the items on this site are retained by the individual author and/or other copyright owners. Users may access full items free of charge; copies of full text items generally can be reproduced, displayed or performed and given to third parties in any format or medium for personal research or study, educational or not-for-profit purposes without prior permission or charge, provided:

- The authors, title and full bibliographic details is credited in any copy;
- A hyperlink and/or URL is included for the original metadata page; and
- The content is not changed in any way.

For more information, including our policy and submission procedure, please contact the Repository Team at: E.mailbox@hud.ac.uk.

<http://eprints.hud.ac.uk/>

Electron paramagnetic resonance evaluation of defects at the (100)Si/Al₂O₃ interface

B.J. Jones^{*} and R.C. Barklie

Department of Physics, Trinity College, Dublin 2, Ireland.

*Tel: +353 1 6082173, Fax: +353 1 6711759, e-mail: b.j.jones@physics.org

PACS codes: 73.20.Hb, 76.30.-v, 77.55.+f

Short Title: EPR Evaluation of defects at the (100)Si/Al₂O₃ interface

Abstract

Electron paramagnetic resonance (EPR) was conducted on aluminium oxide films deposited by atomic layer deposition on (100)Si. Multiplet spectra are observed, which can be consistently decomposed assuming the presence of only P_{b0} and P_{b1} centres, which are well known in Si/SiO₂ structures. Al₂O₃ films deposited on HF-treated (100)Si exhibit unpassivated P_{b0} and P_{b1} centres, with concentrations of $(7.7 \pm 1.0) \times 10^{11} \text{ cm}^{-2}$ and $(8 \pm 3) \times 10^{10} \text{ cm}^{-2}$ respectively. Rapid thermal annealing of the substrate in NH₃ prior to film deposition reduces the unpassivated P_{b0} concentration to $(4.5 \pm 0.7) \times 10^{11} \text{ cm}^{-2}$. Forming gas annealing at temperatures in the range 400°C to 550°C causes no further reduction in defect density; this may be related to a spread in passivation activation energy, associated with low temperature deposition.

1. Introduction

Scaling of metal-oxide-semiconductor (MOS) devices to smaller sizes has so far involved reducing the thickness of the silicon dioxide, SiO₂, oxide layer. However, obstacles such as an increased leakage or tunnelling current set a minimum thickness of oxide below which devices are fundamentally unfeasible [1]. One way to combat this problem is to replace SiO₂ with insulating metal oxides that have a higher dielectric permittivity: aluminium oxide, Al₂O₃, is one material that has emerged as a possible candidate, at least as a short-medium term solution [1, 2].

Al₂O₃ has high thermal stability and therefore, unlike other materials currently under study as SiO₂ replacements, is compatible with the standard CMOS process [3].

However, the quality of the silicon/oxide interface is also of vital importance in MOS devices. Defects at the interface have a detrimental effect on device performance, affecting operational characteristics as well as increasing leakage current and oxide breakdown probability. Therefore a control of interface defects is a critical issue in integrated circuit manufacture [1, 4, 5].

Electron paramagnetic resonance (EPR) is a key tool in atomic-scale identification of point defects and many studies have utilised this technique to examine interface defects in Si/SiO₂ structures [4, 6]. However, little work has been done utilising EPR on aluminium oxide. Stesmans and Afanas'ev [7, 8] use VUV depassivation of defects prior to EPR to show a (100)Si/Al₂O₃ interface that is basically Si/SiO₂-like,

exhibiting both P_{b0} and P_{b1} interface traps. Both P_{b0} and P_{b1} defects are trivalently bonded silicon atoms at the Si/SiO₂ interface, $\bullet\text{Si}\equiv\text{Si}_3$. P_{b0} is axially symmetric about $\langle 111 \rangle$ and P_{b1} has monoclinic symmetry [4, 5]. Both types of defects are of importance from an engineering and material science point of view, and can be passivated (and hence made EPR inactive) through binding with hydrogen at moderate temperatures, thus films deposited in a hydrogen rich ambient would be expected to have low levels of unpassivated defects in their as-deposited state.

Cantin *et al.* [9] show that the P_{b0} and P_{b1} signals observed in EPR studies on Al₂O₃ samples, similar to EPR spectra of silicon dioxide on silicon, are possibly due to a thin, $\sim 0.7\text{nm}$, interface layer of SiO₂. However, TEM measurements have shown that it is possible to deposit Al₂O₃ on silicon without forming an interfacial SiO₂ layer [1]. The same authors also observe an additional isotropic silicon dangling bond, “Si-db”, signal that dominates the EPR spectrum, and suggest that some of this defect is present in the interface or dielectric. They also show that forming gas annealing (FGA) of samples does not produce the decrease in defect density of several orders of magnitude observed in SiO₂ [6], but that the P_{b0} concentration is only reduced by 30-50% [9].

In this study we use electron paramagnetic resonance (EPR) to examine the defects in samples consisting of aluminium oxide that has been deposited by atomic layer deposition (ALD) on (100)Si. We quantify the unpassivated defect density, examine the origin of the Si-db defect, and report on the effects of a pre-deposition nitridation step - which has been shown in a number of dielectrics to improve interface quality

[10, 11] above that of ALD grown films on HF-treated substrates, which may result in uneven nucleation and discontinuous films [10, 12]. We also show the effects of post-deposition annealing in forming gas.

2. Experimental Details

Starting substrates were 200 mm p-type silicon wafers, with resistivity of 20 ohm.cm. After an IMEC clean step, a native oxide etch was performed in 2% HF for 30s. This hydrogen-terminated silicon was one of the substrate surface preparations used in this work (films deposited on this surface are henceforth referred to as “HF-last”). The second surface preparation was a nitridation step performed at 560°C on the hydrogen-terminated silicon by rapid thermal annealing (RTA) in NH₃ for 30s (referred to subsequently as “nitrided”). Al₂O₃ was deposited at Philips by atomic layer deposition (ALD) at 300°C to a thickness of 15 nm, with a tri-methyl alumina (Al(CH₃)₃) precursor.

Some samples were subjected to a 30 minute forming gas anneal (FGA), either at 400°C with a cool down also in forming gas, or a 550°C FGA with a cool down ambient of either nitrogen or forming gas.

The samples for EPR were etched in a CP₄-variant solution to reduce the substrate thickness from 0.5mm to $\approx 150\mu\text{m}$. This reduces the amount of silicon in each sample, and thus decreases the reduction of EPR sensitivity that occurs due to the presence of a conducting material within the cavity. This thinning also allows a

number of 'slices' of a sample to be stacked together in the cavity, increasing the area of interface and volume of bulk film under study. Measurements were typically carried out on bundles of five slices. As a final treatment, the backs and edges of the samples were etched in CP₄-variant solution after cleaving the samples to size, in order to remove the native oxide and passivate the damage centres, respectively. Electron paramagnetic resonance measurements on as-deposited samples were conducted before and after this final etch, to investigate the origin of the Si-db signal. EPR was also carried out on the annealed samples following final etching.

EPR measurements were made at room temperature on a Bruker EMX machine, using 100kHz field modulation, a microwave frequency of approximately 9.9GHz (X-band) and a TM₀₁₁ mode cavity. Each g value was calculated by comparing the field position of the resonance with that of a resonance of known g value, in this case F⁺ centres in MgO, with g=2.0023. The field range was calibrated with a proton NMR probe that also gave absolute field values.

Measurements were conducted at a non-saturating power. To improve the signal-to-noise ratio without distorting the EPR line, each spectrum has been averaged over a large number of scans with the modulation field kept at approximately one third of the P_{b1} peak-to-peak linewidth, the narrowest feature in each spectrum [13]. Errors given in this work are suitable for comparing one sample with another on this set-up – but do not include error in Varian standard concentration or measurement. For absolute uncertainty values fractional errors should be increased by approximately 20%.

3. Results and Discussion

3.1 Si-db centre

Figure 1 shows EPR spectra of the as-deposited HF-last film, prior to the final etch of the substrate back and edges. Figure 1 a) and b) show the spectrum obtained when the applied field is parallel to the [100] and [111] direction, respectively. The spectra are clearly asymmetric, and in addition to lines with position dependent on field orientation, a resonance line with isotropic g value, $g \approx 2.0056$, is clearly observed. Previous work [9] has shown that such a resonance line can be present in addition to the lines due to P_{b0} and P_{b1} defects. This line is attributed to silicon dangling bonds (Si-db) and is well known to occur in damaged silicon [14]. The fit to these spectra, included in figure 1, shows each spectrum can be accurately decomposed into components, and consists of only Si-db, P_{b0} and P_{b1} lines.

Figure 2 shows spectra taken from repeating the EPR measurements after the etch to remove oxide from the back of the wafer and to passivate damage on cleaved edges. It can be immediately seen that although there is a line with $g \approx 2.0056$ in the [100] spectrum, there is no corresponding line in the [111] spectrum. This suggests that the isotropic Si-db line has been removed by the etching process, and the lines observed in the [100] spectrum are anisotropic P_{b0} and P_{b1} lines. This hypothesis can be verified by fitting to the experimental spectra.

In all cases the EPR spectra taken with field in [100] direction, after the final etch, can be decomposed into component lines assuming only the presence of P_{b0} and P_{b1} type defects. To verify that only these defects are present, fits are made to the spectra taken with the magnetic field in the [111] orientation using the relative intensities of P_{b0} and P_{b1} taken from [100] fits. Fitting to the [111] spectra shows that there is no resonance line with isotropic g-value at $g \approx 2.0056$, and thus indicates that the signal in [100] is due to P_{b0} , not silicon dangling bonds, and in addition shows that the intensities obtained from [100] fit are consistent with the spectra obtained at another orientation. The absence of the isotropic line at $g \approx 2.0056$ is shown to be due to the etch immediately prior to conducting the EPR measurements. This etch removes any signal due to damage and oxide growth on the back of the substrate and on the lateral cleavage planes – thus EPR spectra can be collected without the resonance line due to the Si-db centre that is observed to be obscuring the P_{b0} signal in recent work by Cantin *et al.* [9].

3.2 P_{b0} and P_{b1} centres

P_{b0} and P_{b1} concentrations and linewidths are obtained through fits made to the (derivative) spectrum taken with the magnetic field in the [100] direction (i.e. perpendicular to the sample, for these films on (100)Si substrates). These fits assume Lorentzian lines fixed at, or within error of, the known g-values for P_{b0} and P_{b1} in this field orientation, $g=2.0059$ and $g=2.0037$, respectively [7, 9]. With the applied field in this orientation the four branches coincide for both P_{b0} and P_{b1} thus making identification and measurements more accurate. The intensities of the resonance lines

are calculated from the height multiplied by the square of the peak-to-peak linewidth, with appropriate normalisation and shape factor corrections. The defect concentration is then calculated by comparing the intensity to that of a standard Varian sample of pitch in KCl. The total defect concentration is then the sum of the concentrations of individual defect types.

The P_{b0} and P_{b1} defect densities and component linewidths obtained from fitting to $B \parallel [100]$ spectra are shown in table 1. Sample spectra from measurements with $B \parallel [100]$ and $B \parallel [111]$ are shown in figure 2a and figure 2b, respectively, fits consisting of P_{b0} and P_{b1} component lines are also shown.

Anneal conditions	Surface	$[P_{b0}] / 10^{11} \text{cm}^{-2}$	$\Delta B_{pp} / G$ P_{b0}	$[P_{b1}] / 10^{10} \text{cm}^{-2}$	$\Delta B_{pp} / G$ P_{b1}	Total Defects / 10^{11}cm^{-2}	$[P_{b0}] / [P_{b1}]$
None	HF-last	7.7 ± 1.0	3.5(1)	8 ± 3	2.4(2)	8.5	10
	Nitrided	4.5 ± 0.7	4.0(3)	11 ± 5	2.2(3)	5.6	4
400°C FG Cool	Nitrided	5.8 ± 0.9	3.3(1)	5.8 ± 2.1	2.2(2)	6.4	10
550°C N ₂ cool	HF-last	5.8 ± 0.9	4.9(1)	3.2 ± 0.9	2.0(2)	6.1	18
	Nitrided	5.3 ± 0.8	3.4(1)	39 ± 7	3.5(1)	8.2	1.3
550°C FG cool	HF-last	6.4 ± 0.9	4.0(1)	≤ 6.6	2.6(3)	6.7	10
	Nitrided	4.6 ± 0.6	3.5(1)	5.7 ± 1.6	2.5(1)	5.2	8

Table 1. Concentrations of EPR-active centres for Al₂O₃ films on “Nitrided” (NH₃) and “hydrogen-terminated” (HF-last) substrates. Peak-to-peak linewidths for $B \parallel [100]$ are also shown. All anneals were carried out in forming gas (FG) with cool down either in FG or N₂.

The as-deposited film grown on the hydrogen terminated substrate shows a concentration of unpassivated P_{b0} defects of $(7.7 \pm 1.0) \times 10^{11} \text{ cm}^{-2}$. This is approximately one order of magnitude lower than the $\sim 6 \times 10^{12} \text{ cm}^{-2}$ defects after depassivation by photodesorption, observed by Stesmans and Afanas'ev [7] in their work on (100)Si/Al₂O₃/ZrO₂ stacks grown by ALD on substrates treated with a HF dip prior to deposition. The P_{b1} defect concentration is, at $(8 \pm 3) \times 10^{10} \text{ cm}^{-2}$, approximately a factor of ten smaller than the P_{b0} concentration seen in the as-deposited films in the current work. This dominance of P_{b0} over P_{b1} is also observed in Cantin's work [9] and in Stesmans' and Afanas'ev's [8] depassivated films; it probably reflects the rather low deposition temperature, since high [P_{b0}]/[P_{b1}] ratios are also seen in SiO₂ films grown with low oxidation temperatures (T_{ox}). Thermal SiO₂ grown at T_{ox} = 180 °C has concentrations of defects such that [P_{b0}]/[P_{b1}] ≈ 20; this ratio decreases as the oxidation temperature is raised [15].

It is worth noting that the P_{b0} and P_{b1} linewidths obtained from the fits to spectra in this work are, at $4.1 \pm 0.8 \text{ G}$ and $2.2 \pm 0.2 \text{ G}$ respectively, considerably smaller than the $9.7 \pm 0.4 \text{ G}$ and $3.75 \pm 0.2 \text{ G}$ observed in (100)Si/Al₂O₃/ZrO₂ stacks by Stesmans and Afanas'ev [7].

It can be seen from table 1 that the initial nitridation step reduces the detected P_{b0} concentration for as-deposited films, from $(7.7 \pm 1.0) \times 10^{11} \text{ cm}^{-2}$ to $(4.5 \pm 0.7) \times 10^{11} \text{ cm}^{-2}$. This suggests that the NH₃ RTA reduces the number of P_{b0} defects or causes further passivation. This is consistent with previous electrical measurements on aluminium

and zirconium oxide on silicon, which show that nitridation of the silicon substrate produces a better quality interface [10, 11].

Forming gas annealing (FGA) of SiO₂ films on silicon causes the P_b-type defect concentration to be reduced by several orders of magnitude [6]. However, annealing of our nitrided Al₂O₃ film in forming gas at 400°C causes no further reduction in the concentration of detected unpassivated defects. This contrasts with the effect of FGA on SiO₂, but matches (in context) with the reduction of only ~30% in P_{b0} concentration following a 450°C FGA observed by Cantin *et al.* [9] in their work on ALD Al₂O₃ films deposited on HF-dipped (100)Si. However, this may be because a large proportion of the P_{b0} and P_{b1} defects are already passivated in the as-deposited state. Indeed the defect concentrations in the as-deposited films in this work are similar to the lowest observed by Stesmans and Afanas'ev [8] in their trials of various post-deposition treatments.

The lack of passivation efficiency is perhaps related to the low-temperature deposition conditions. Work on SiO₂ [16] has shown that for fixed anneal conditions, defects in films produced with low oxidation temperatures, T_{ox}, of 250°C are passivated to a much lesser extent than films with a higher T_{ox}. This is attributed to higher levels of interface stress in these low temperature films, which leads to a variation in P_b morphology between individual sites, creating a spread in the passivation activation energies [16, 17]. This results in a proportion of sites, with high activation energies, that are not passivated by a standard anneal. The ALD process at 300°C, which in some cases essentially creates a low-T_{ox} SiO₂ interface [1, 9], may also produce films

with levels of interface stress that cause significant spread in the passivation activation energy of P_b centres, which therefore causes the passivation efficiency to be reduced.

Forming gas annealing at 550°C with cool down in nitrogen, causes the P_{b1} concentration of the nitrified film to increase from $(1.1 \pm 0.5) \times 10^{11} \text{ cm}^{-2}$ to $(3.9 \pm 0.7) \times 10^{11} \text{ cm}^{-2}$, approaching the $(5.3 \pm 0.8) \times 10^{11} \text{ cm}^{-2}$ of P_{b0} defects. This decrease in the [P_{b0}]:[P_{b1}] ratio following our 550°C anneal may initially suggest a relaxation of the interface stress. However, with an anneal at 550°C but with a cool down in forming gas, the defect concentrations and relative intensities are very similar to those of the unannealed sample, and have not been reduced as would be expected following stress relaxation. It is probable that the relatively high anneal temperature is beginning to drive hydrogen off defect sites where it is more weakly bound, thus depassivating a proportion of the defects. The cool down in nitrogen will cause these defects to remain unpassivated, however, cooling down in forming gas has allowed hydrogen in the ambient to repassivate the defects.

4. Conclusions

EPR measurements on (100)Si/Al₂O₃ show the presence of unpassivated P_{b0} and P_{b1} defects, similar to those observed in Si/SiO₂ interfaces. For as-deposited films on hydrogen terminated (HF-last) surfaces the P_{b1} concentration is $(8 \pm 3) \times 10^{10} \text{ cm}^{-2}$; however, the P_{b0} line dominates the spectra with a concentration of $(7.7 \pm 1.0) \times 10^{11} \text{ cm}^{-2}$. This is an order of magnitude smaller than the concentration of defects following

depassivation [7]. No isotropic line due to damage-related silicon dangling bonds (Si-db) is observed, contrary to inference in another work [9], confirming that for our ALD samples this defect is wholly in the lateral cleavage planes and/or substrate back.

Subjecting the substrate to an RTA in NH₃ prior to film deposition is shown to reduce the P_{b0} density to $(4.5 \pm 0.7) \times 10^{11} \text{ cm}^{-2}$, however, no further reduction of density (within errors) occurs following forming gas annealing at temperatures in the range 400°C to 550°C. We suggest that the lack of passivation efficiency may be the result of a spread in passivation activation energies, caused by stress levels in the interface associated with low temperature deposition. This reduced annealing passivation efficiency and the high [P_{b0}]/[P_{b1}] ratio seen in these films are also observed in thermal SiO₂ grown with low oxidation temperatures [15, 16]. The effects seen are perhaps, therefore, associated with a SiO₂ interface layer.

5. Acknowledgements

This work is supported by Higher Education Authority of Ireland's PRTL I programme, and by Trinity College Dublin. The authors would like to thank J.C.Hooker of Philips Research, Leuven, Belgium for supplying films, and acknowledge the assistance of P.K. Hurley and B.J. O'Sullivan of NMRC, Cork, Ireland.

References

- [1] G.D. Wilk, R.M. Wallace and J.M. Anthony *J. Appl. Phys.* 89 (2001) 5243
- [2] E. P. Gusev, M. Copel, E. Cartier, I. J. R. Baumvol, C. Krug and M. A. Gribelyuk *Appl. Phys. Lett.* 76 (2000) 176
- [3] D.A. Buchanan, Presented at “13th Workshop on Dielectrics in Microelectronics” June 2004 Kinsale, Co. Cork, Ireland.
- [4] A. Stesmans and V.V. Afanas'ev *J. Appl. Phys.* 83 (1998) 249
- [5] M.L. Reed and J.D. Plummer *J. Appl. Phys.* 63 (1988) 5776
- [6] A. Stesmans *Appl. Phys. Lett.* 68 (1996) 2076
- [7] A. Stesmans and V.V. Afanas'ev *J. Phys C* 13 (2001) L673
- [8] A. Stesmans and V.V. Afanas'ev *Appl. Phys. Lett.* 80 (2002) 1957
- [9] J.L. Cantin and H.J. von Bardeleben *J. Non-Cryst. Sol.* 303 (2002) 175
- [10] W. Tsai, R. J. Carter, H. Nohira, M. Caymax, T. Conard, V. Cosnier, S. DeGendt, M. Heyns, J. Petry, O. Richard, W. Vandervorst, E. Young, C. Zhao, J. Maes, M. Tuominen, W. H. Schulte, E. Garfunkel and T. Gustafsson *Microelectron. Eng.* 65 (2003) 259
- [11] R.T. Brewer, M.-T. Ho, K.Z. Zhang, L.V. Goncharova, D.G. Starodub, T. Gustafsson, Y.J. Chabal and N. Moumen. *Appl. Phys. Lett.* 85 (2004) 3830
- [12] M. Copel, M. Gribelyuk and E. Gusev *Appl. Phys. Lett.* 76 (2000) 436
- [13] R.C. Barklie, M. Collins and S.R.P. Silva *Phys. Rev. B* 61 (2000) 3546
- [14] G.K. Walters and T.L. Estle *J. Appl. Phys.* 32 (1961) 1854
- [15] D. Pierreux and A. Stesmans *Phys. Rev. B.* 66 (2002) 165320
- [16] A. Stesmans *J. Appl. Phys.* 92 (2002) 1317
- [17] K.L. Brower *Phys. Rev. B.* 38 (1988) 9657

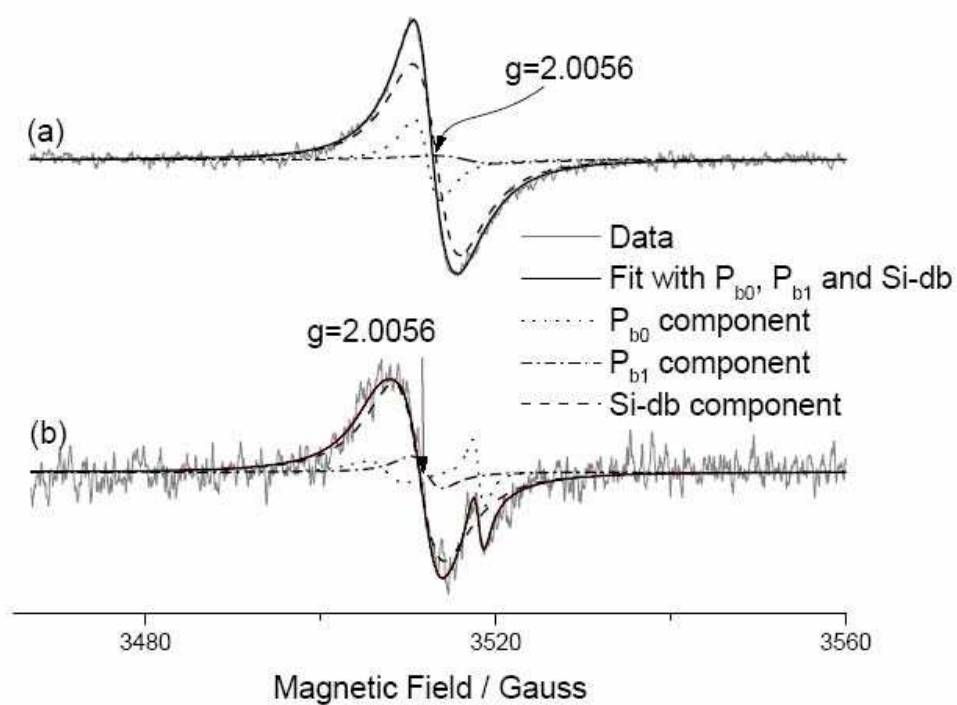


Figure 1. EPR spectra of as-deposited HF-last Al₂O₃ sample, with applied magnetic field a) parallel to [100] and b) parallel to [111].

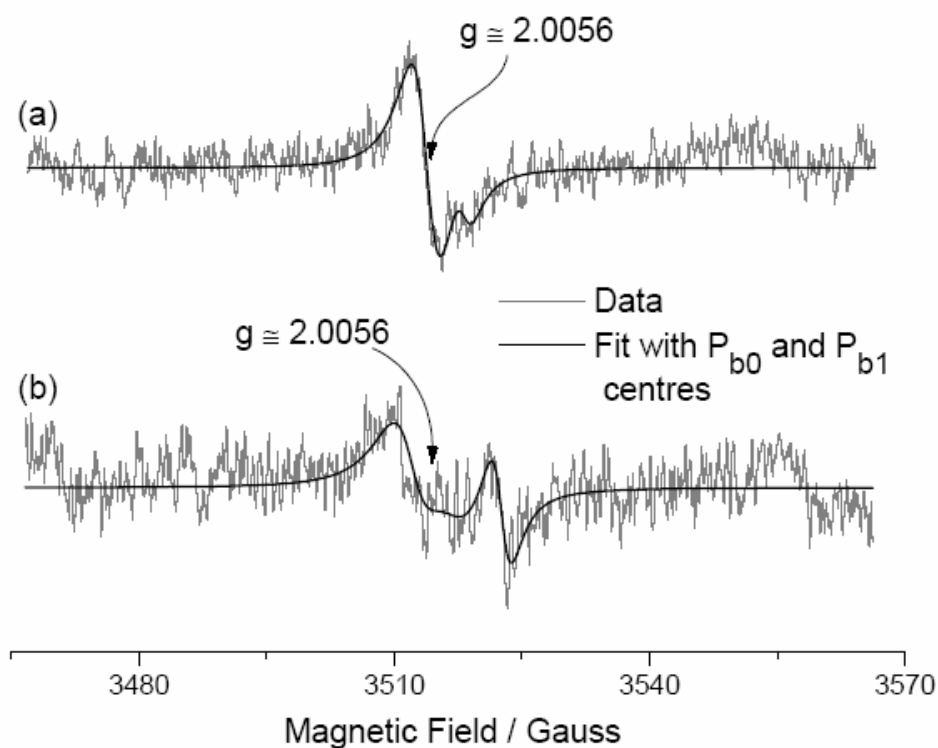


Figure 2. EPR spectra of Al₂O₃ films on hydrogen-terminated silicon substrates, after etch of wafer back and cleavage planes, with applied field in a) [100] and b) [111] directions